



# Cardiovascular-interventional-surgery virtual training platform and its preliminary evaluation

Chaozheng Zhou<sup>1</sup>

Le Xie<sup>1,2\*</sup>

Xianglong Shen<sup>1</sup>

Maisheng Luo<sup>3</sup>

Zhaoli Wu<sup>1</sup>

Lixu Gu<sup>3</sup>

<sup>1</sup>*Institute of Forming Technology & Equipment, Shanghai Jiao Tong University, Shanghai 200030, China*

<sup>2</sup>*National Digital Manufacturing Technology Center, Shanghai Jiao Tong University, Shanghai 200030, China*

<sup>3</sup>*Department of Biomedical Engineering, Shanghai Jiao Tong University, Shanghai 200030, China*

\*Correspondence to: Le Xie, National Digital Manufacturing Technology Center, Shanghai Jiao Tong University, Shanghai, China.  
E-mail: lexie@sjtu.edu.cn

## Abstract

**Background** Cardiovascular interventional surgery (CIS) training has mainly been performed with fluoroscopic guidance on animals. However, this has potential drawbacks, including from the anatomical differences between animal models and the human body. The purpose of this research is to develop a virtual training platform for inexperienced trainees.

**Methods** The CIS virtual training platform is composed of a mechanical manipulation unit, a simulation platform and a user interface. A decoupled haptic device offers high-quality force feedback. An efficient physically based hybrid model was simulated. The CIS procedure was tested with three simulation studies.

**Results** Translational and rotational tests were employed to preliminarily evaluate the platform. Tests showed that accuracies improved by 50% and 32.5%. Efficient collision detection and continuous collision response allowed real-time interactions. Furthermore, three simulation studies indicated that the platform had reasonable accuracy and robustness.

**Conclusions** The proposed simulation platform has the potential to be a good virtual training platform. Copyright © 2014 John Wiley & Sons, Ltd.

**Keywords** cardiovascular interventional surgery; haptic device; real-time interactions; force feedback

## Introduction

Cardiovascular disease is the leading cause of death in China and the world. Vascular Interventional Surgery (VIS), also referred to as Vascular Interventional Radiology (IR), is an alternative to open surgery. VIS is a minimally invasive surgical procedure that uses X-ray imaging (C-arm) to supervise the manipulation of instruments, such as needles, guidewires and catheters in a patient's vascular system. It also extends diagnostic procedures for therapy (most commonly angiographies with contrast agent injection) of cardiovascular diseases. Effective treatment of cardiac diseases is possible through procedures utilizing local anesthesia, catheter balloon inflation (angioplasty), stent placement (1), as well as other fascinating treatments, including that proposed by Rebholz *et al.* (2). A VIS procedure begins with the Seldinger technique, and

Accepted: 15 September 2014

guidewires and catheters are then manipulated through the needle. Once the guidewire is securely located within the vessel, a catheter is manipulated over the guidewire. VIS has become a fundamental protocol due to its minimally invasive nature, shorter in-hospital and recovery times and lower medical costs. Furthermore, VIS with dexterity and real-time monitoring results in significantly higher performance in treating various endovascular diseases, compared with conventional open surgery.

Traditionally, VIS has been taught using the master–apprentice model, with additional training on animals or mock models, which have the advantages of similarity, typicality, and repeatability. However, these methods have several drawbacks, including ethical concerns, radiation exposure and high costs. In addition, the similarity is inconsistent with clinical practice or there is a conflict between similarity and typicality. Virtual training is employed to solve these problems owing to its simulation, autonomy, and security. Furthermore, patients are at risk during the period when trainees first begin their specialization. Due to difficult hand–eye coordination, complicated manipulation (e.g. translation, rotation) of the instruments and the risk of vessel injury, surgeons can continuously enhance their own skills with repeated training. Moreover, the virtual environment protects trainers from the risks of practical training, and trainers may gain perceptual knowledge and practical experience through this training. Thus, a computer-based CIS virtual training platform was implemented to allow realistic and adapted training for trainees.

Accordingly, VIS robotic virtual training systems have developed rapidly and generated many commercial simulations during past decades. One of the early commercial simulations was the virtual interventional radiology procedure (VIRP) system (3), which provided simulation in true blood vessels with two-dimensional (2D) motion. Although successfully performed as a viable study, the surgeons could not feel realistic forces because of the poor precision in measurements. The Mentice Vascular Interventional System Trainer (4) is another example of a virtual interventional system. These two robotic systems employed the contact-type displacement measurement system and therefore could not provide realistic tactile force feedback. The ANGIO Mentor (5,6) was the first non-contact displacement measurement system with applications in VIS. Ilic and Moix *et al.* (7,8) proposed a computer-assisted haptic simulator with real-time visualization and force feedback for interventional radiology procedures. They accurately reproduced the force and torque dynamic experienced during a real procedure, by using a haptic simulator to perform virtual reality colonoscopy simulations. Several clinical studies (9–13) have been dedicated to real-time simulations training core skills in vascular interventional procedures.

In addition, several groups have focused on realistic visualization and guidewire modeling in recent years. Luboz *et al.* (14) proposed a hybrid mass–spring model to simulate a guidewire with a set of particles connected by rigid springs of fixed lengths; however, this model cannot simulate an inherent bending guidewire. Another relatively accurate model (15) based on energy minimization and optimization technique has been proposed but is not satisfactory even with the use of an accelerating algorithm. Lenoir *et al.* (16) developed an incremental finite beam element model without resolving the global stiffness matrix, which could reduce the computational time and make real-time interaction possible. Duratti *et al.* (17) presented an interventional radiology system based on the Cosserat rod model to address the nonlinear deformation of the guidewire. Other non-Cosserat rod approaches (e.g. graph-theoretical method, minimal total potential energy method) were expected to predict the catheter's tip position, assuming that the catheter bends with zero torsion and with constant curvature (18,19). Tang *et al.* (20) applied an implicit time integration method to the Kirchhoff elastic rod model for guidewire simulation. Although these studies proposed diverse real-time models with realistic visualization and catheter modeling integrated into a complete system, some still have the drawback of requiring the use of modified instruments, high inertia of the haptic feedback and coupled or passive force feedback. Thus, taking into account all of these details is still a challenging task.

We have designed a cardiovascular interventional surgery (CIS) virtual training platform with rapid and accurate response force feedback and thus have created a realistic simulated environment for training core techniques to trainees. Compared with the above intervention training systems, our virtual training platform has three improvements. First, our decoupled haptic device offers superior dynamic behavior and low inertia of the force feedback, which delivers a realistic simulation environment to the trainees. In addition, we deploy an efficient physically based hybrid model which can realistically and interactively simulate the complex behaviors of guidewires and catheters. Finally, our simulation platform allows for the testing of VIS principles, such as guidewire and catheter simulation and stent placement as well as rendering techniques for realistic simulation.

In this paper, we first focus on the core technologies (e.g., mechanical design system and guidewire modeling) of the CIS virtual training platform. After that, the control system is briefly introduced. Then, we investigate the system performance through experimental tests and evaluate the feasibility of our platform through preliminary tests. Finally, we discuss the experimental results and future work.

## Materials and methods

The CIS virtual training platform consists of three parts: a mechanical manipulation unit, a simulation platform and a user interface (Figure 1). The mechanical manipulation unit includes a mechanical design module, a balloon pump module and an injector module. The mechanical design module qualifies the motion (translation, rotation) as master manipulation, while the control system reproduces it with a program-designed scaling ratio as slave manipulation displayed on the computer screen, which can be manipulated with high precision. In addition, the other two surgical instruments are used to test pressure and flow, respectively. The simulation platform uses two computers working together, one for real-time image navigation and the other for monitoring the operating status of the control system. In this way, we can simultaneously control the process of real-time simulation surgery and the operation status of the mechanical system.

Two decoupled measuring mechanisms (Figure 2) have been developed, allowing the axial and rotating forces to be perceived and measured separately. The translational force feedback mechanism, fixed at the entrance of angiographic catheter module, measures the translational movements and applies force feedback. The rotational force feedback mechanism is perpendicular to the translational arrangement, and measures the rotational movements and provides force feedback accordingly. This modular design has a mechanism arrangement similar to the other two modules (i.e. guidewire module, coronary dilatation catheter module). The mechanical design system generates translational and rotational motions of the interventional instruments with the help of sensors, while the control system receives the data in order to regenerate the similar motion with the help of rendering techniques. The mechanical system is controlled by a real-time control system, which ensures an efficient force feedback response. A real-time, physically based modeling

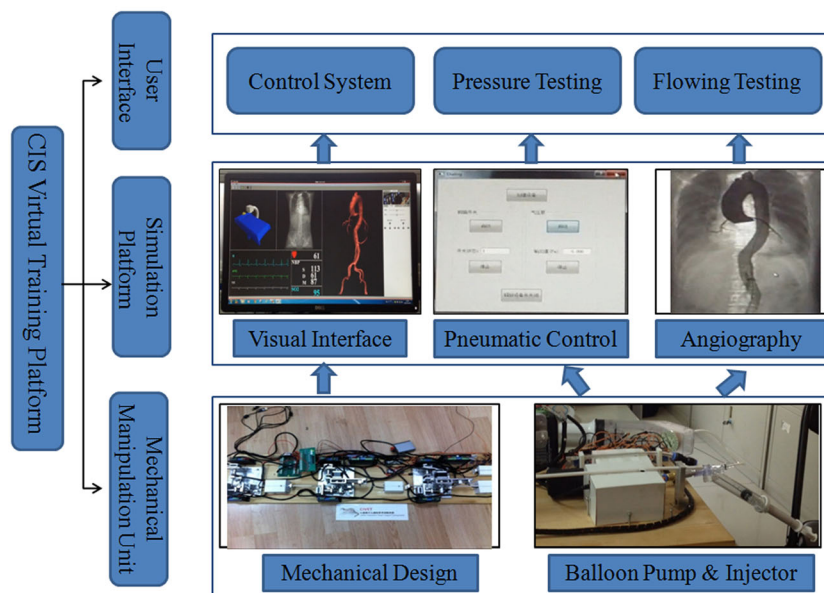


Figure 1. The CIS training platform

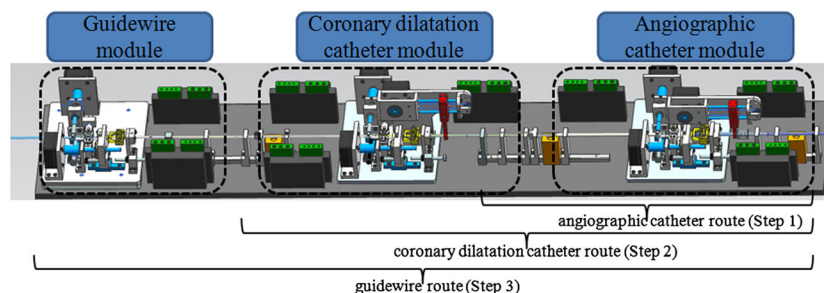


Figure 2. Routes of angiographic catheter, coronary dilatation catheter and guidewire in the mechanical system

approach is proposed to simulate complicated behaviors of guidewires and catheters as well as an adaptive sampling algorithm for simulation efficiency without reducing accuracy. Thus, it is possible to neglect the delay time considering the reliable response and timely data updating. In our configuration, a pedal was implemented for emergency situations or to restart the control system after repositioning.

The simulation platform, which provides efficient collision detection and collision response, uses two computers working together, one for real-time image navigation and the other for monitoring the operating status of the control system allowing for simultaneous control of the process of real-time simulation surgery and the operation status of the mechanical system. The virtual catheterization is rendered with a real-time frame rate of 75 FPS with a single high-performance instrument. The guidewire model uses up to 800 particles, interacting with a highly detailed vascular model of almost 90 000 polygons from a 20-patient database. Our simulation was tested on a PC with Intel(R) Xeon(R) E3-1230 V2 3.3GHz CPU and an Nvidia GeForce GTX 760 GPU.

The user interface (see later Figure 13(b)) is composed of three parts: visualization, vascular modeling, and guidewire/catheter simulation. The visualization includes a virtual operation scene, a CT image and a virtual ECG monitor developed to simulate the realistic virtual operation environment. The vascular model is constructed based on the segmented blood vessels obtained from CT images (data from Southern Medical University), where the aorta and coronary arteries was achieved via a semi-automatic algorithm (21). The vascular model is fed into the guidewire/catheter simulation for collision detection between instruments and vessel walls. The user's manipulations and movements (e.g. pushing, pulling and twisting) are captured by sensors and the output force is fed back to them.

## Mechanical design system

The mechanical design system was developed according to clinical requirements and the force feedback mechanism. It is composed of a guidewire control module, a coronary dilatation catheter module and an angiographic catheter module (Figure 2). Each sub-module has two haptic devices, one for translational force feedback and the other for rotational force feedback. A guiding device was designed and mounted on each module to smoothly and precisely deliver the interventional instruments from the previous module to the next. Based on this configuration, independent active force feedback as well as rotational and translational movements can accurately be obtained. We divided the CIS simulation procedure into

three steps. The first step was puncturing with the angiographic catheter and the aim was to establish a channel to the lesions and stabilize the operation of the guidewire. The second step was catheter modification and the aim was to match the proximal blood vessel with good coaxial conditions to obtain better symmetric external blood pressure. The third step was the guidewire process. On account of the established channel, the guidewire can be smoothly and stably sent to the lesions without excessive resistance. Depending on the characteristics of the lesions and the diameters of blood vessels, we choose the guide wire head with a specific camber size. In cases of narrow lesions, we rotate and push forward the guidewire simultaneously. Finally, based on the above operations, we push the coronary dilatation catheter slowly along the guidewire to the lesions. Most importantly, we fix the guidewire to avoid vascular injury when inserting.

Figure 2 illustrates the routes of the angiographic catheter, the coronary dilatation catheter and the guidewire in the mechanical design system. To further introduce the characteristics of each module unit, we designed three routes for the CIS simulation procedure considering the differences in diameter size. The displacement of each route is tabulated in Table 1.

## Design of force feedback module

For the CIS simulation procedure, we employed three similar structural arrangement modules. Each module is mechanically divided into three sub-modules: the translational force feedback module, the rotational force feedback module and the steering-guided module (Figure 2). The translational and rotational force feedback module measures the translational and rotational movements and applies force feedback, respectively. Accordingly, the steering-guided module was made for smoothly and precisely delivering the interventional instruments from the previous module to the next one. When the inserted instrument (e.g. catheter, guidewire) is in a suitable place, it is held by the gripper mounted on the rod between the two cylinders in a friction drive arrangement (Figure 3). The first cylinder is attached to a DC motor in direct drive, thus applying active force feedback for the translational movement. The whole steering-guided system is linked with a belt to a second DC motor.

**Table 1.** Displacement range of each route

Type of route	Displacement range (cm)	
	Minimum	Maximum
Angiographic catheter	0	60
Coronary dilatation catheter	0	90
Guidewire	0	120



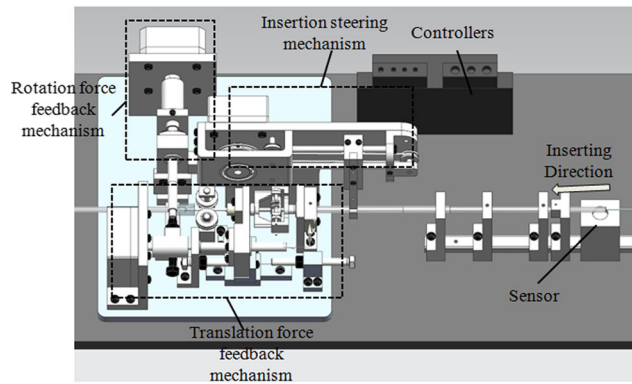


Figure 3. Details of one module of the platform

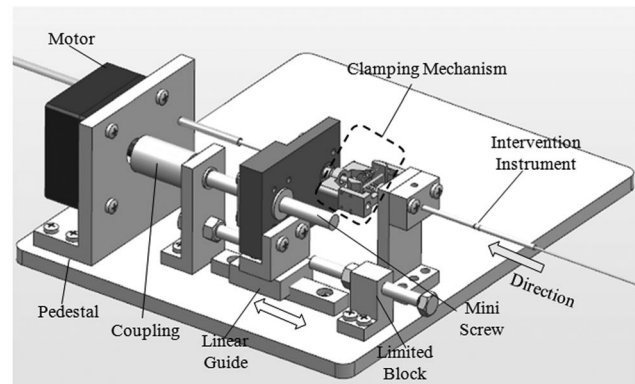
Both cylinders are coated with rubber to increase friction, hence avoiding slippage between the instruments and the cylinders. The details of other two sub-modules are further discussed in the following sections.

### Translational and rotational force feedback mechanism

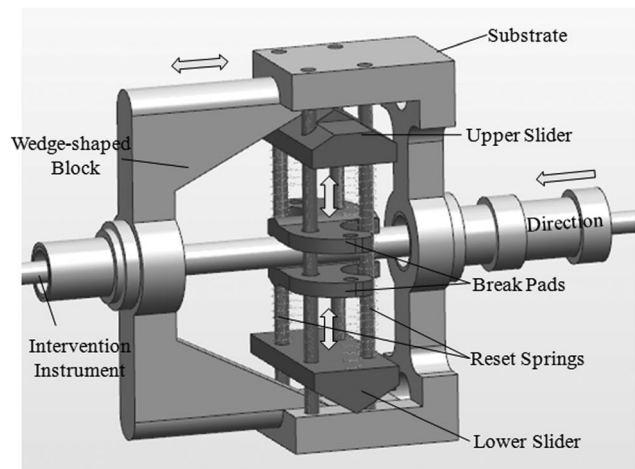
The proposed mechanism is a new and original approach to achieve high-quality haptic force feedback with lower inertia and friction to the system. This mechanism is mainly comprised of a stepper motor, coupling, mini-screw, linear mini-guide and a clamping mechanism (Figure 4(a)). When the stepper motor is started, the mini-screw coupling the linear guide translates the rotational motion into translational motion. Then, the wedge-shaped block of the clamping mechanism (Figure 4(b)) mounted on the linear guide moves following the axial direction. Once the breaking pads are in a specific place, they apply force on the interventional instrument. The friction can be neglected due to the low coefficient of friction between the interventional instrument and the precision rollers. Hence, it is possible to measure the translational force and efficiently feed this back to the trainees as soon as it is contacted with the breaking pads.

The rotational mechanism has a similar structure and identical principle (Figure 5) to the translational force feedback mechanism. The only difference is in the clamping mechanism, which implements two precision rollers that apply rotational force. The rotational force can be accurately measured because of the light weight of the translational clamping mechanism inertia and the precise transmission to the trainees. The forward force is negligible because of the low coefficient of friction between the interventional instrument and the precision roller. However, the rotating force is noticeably perceived.

To our knowledge, the CIS simulation does not present a single translational or rotational force feedback simulation, but mostly encounters it with a complicated state. Table 2 lists the parameters of some important parts.



(a)



(b)

Figure 4. Translational force feedback CAD model (a) and clamping mechanism (b)

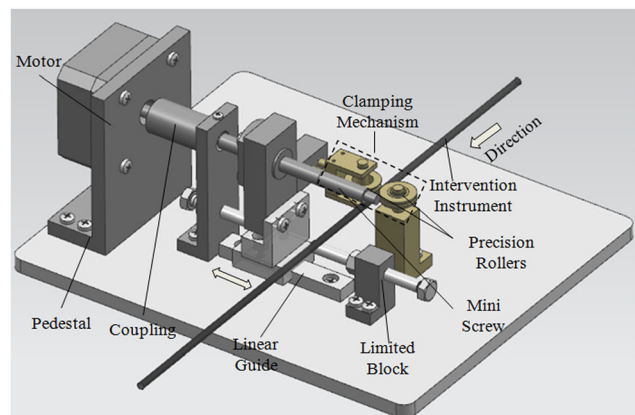


Figure 5. Rotation force feedback mechanism

### Force and torque sensing measurement

A customized force sensor, illustrated in Figure 6(a), is integrated in the clamping mechanism to measure the

Table 2. Parameters of some important parts

Name	Type	Material	Manufacturer
Source material	6061 AL Alloy	Al-Mg-Si	ALCOA
Stepper motor	ACT 14HS	Stainless steel	ACT MOTOR
Mini screw	MSSRA	SUS304	MISUMI
Linear guide	SSEBS	Stainless steel	MISUMI
Ceramic bearing	SKF ABEC-9	ZrO2	MISUMI

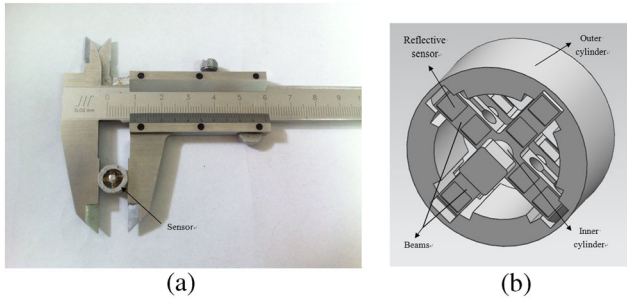


Figure 6. Prototype of the customized sensor (a) and its complete arrangement (b)

translational and rotational force using closed-loop control architecture. The measurement is converted to a deformation of a mechanical structure. The deformation is measured by reflective sensors. The mechanical structure of the sensor is composed of two cylinders connected with four beams on which four reflective sensors are fixed. The inner cylinder is fixed to the main frame in direct measuring form while the outer cylinder is attached to the motor. The stiffness of the structure is very high in all directions except for the axial one. The complete arrangement is presented in Figure 6(b). When a perpendicular force or a torque is applied, the beams deflect and the deflection is measured by reflective sensors. Furthermore, the output signals are added to eliminate unwanted perturbations.

The resolution of the measured force and torque of the catheter, estimated for a 6 F (1 F = 1/3 mm), is 0.02 N over ±10 N and 0.035 mNm over ±15 mNm. However, the force and torque resolution should be of 0.02 N and 0.04 mNm to meet human sensory system (22). Thus, our CIS simulation should be possible to perform.

### Guidewire simulation module

The guidewires and catheters used in the vascular intervention simulation are modeled by thin, fixed centerlines. The centerline, surrounded by finite thin elastic material, can be bent but not stretched. It is a challenging task to realistically simulate the complicated behaviors of guidewires in an interactive manner.

The configuration of guidewire of length  $L$  is described as an adapted framed curve  $\Gamma = (\gamma; n_1, n_2, n_3)$  (Figure 7(a)). Here  $\gamma(u, t)$  represents the rod's centerline curve, with the material coordinate  $u \in [0, L]$  along the centerline and time  $t$ . The material frame  $(n_1, n_2, n_3)$  is a right orthonormal basis attached to each mass point along the centerline, containing the requisite information for measuring bending and twisting of the guidewire. This material frame satisfies  $n_1(u, t) \perp n_2(u, t)$ ,  $n_2(u, t) \perp n_3(u, t)$ ,  $n_1(u, t) \perp n_3(u, t)$ ,  $n_1(u, t) = \gamma'(u, t) / |\gamma'(u, t)|$ . The length of the spatial derivative  $|\gamma'(u)|$  indicates the stretch of the centerline  $\gamma(u)$ . Without loss of generality, we assume the length of the rod to be 1. As a consequence,  $|\gamma'(u)| = 1$  if the rod is inextensible. We formulate the elastic energy based on the Kirchhoff elastic rod (23). However, the geometric configurations and mechanical properties of the guidewire tip are distinguished from that of the main slender body, where the same simulation models were applied throughout the whole guidewire. It is computationally inefficient especially when the nonlinear deformation model suffers

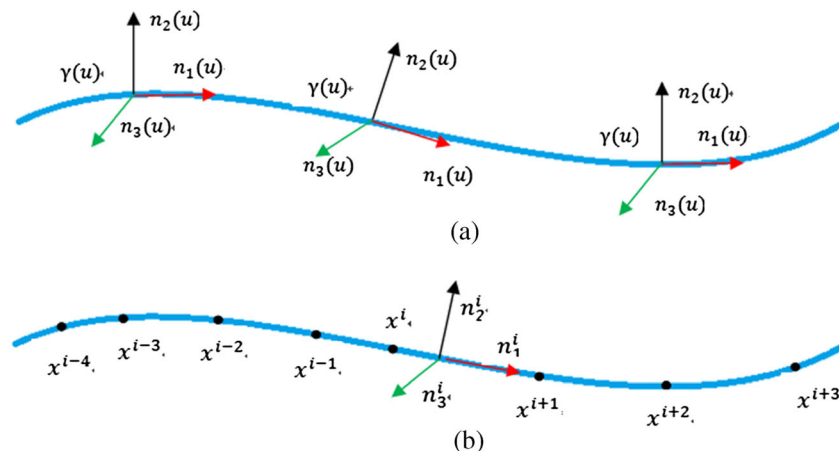


Figure 7. Guidewire resprented by a curve  $\gamma(u)$  and the material Frame  $(n_1, n_2, n_3)$  (a) and Continuous guidewire can be discretized as a discrete one with n segments (b)

from real-time performance issues. We use a less expensive special case of naturally straight, isotropic Kirchhoff rods rather than the generalized Kirchhoff rods for flexible tip modeling the slender body of the guidewire, which is computationally efficient and effective.

In order to maintain the real-time simulation speed while at the same time ensuring the guidewire's sampling resolution, we presented an adaptive sampling strategy that dynamically modified the discrete setting of the guidewire (Figure 7(b)) according to the shape of the guidewire during the insertion. It splits the edges of the guidewire into smaller edges when the curvature of the guidewire is large. However, the length of these edges is not small enough to describe the guidewire behavior more precisely. On the other hand, merging the small edges of the guidewire into larger edges reduces computation when the curvature of the guidewire is small. Figure 8 shows a more detailed principle of the adaptive sampling.

## Collision detection and response

In CIS, collisions between the guidewire and interior vessel walls should be detected. To prevent the guidewire from penetrating through the vessel walls, every collision must be detected at every time-step. Thus, the reaction force can be calculated as an external force. The bounding-volume hierarchy method (BVH), which can logarithmically reduce the time complexity, is an efficient collision detection algorithm. We only update the deformation of the guidewire during the simulation because the deformation of arteries is considered to be very small. Hence, we enwrap the rod model volume with spheres and vessel walls with discrete

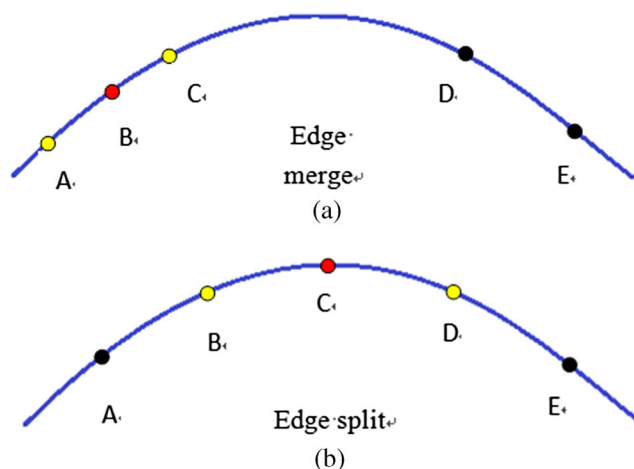


**Figure 8.** Adaptive sampling of the guidewire (a) AB and BC are merged to form large edge AC. (b) BD is divided into two edges BC and CD

orientation polytopes (k-dops) (24), and the k value of the optimal execution performance is 18 in our simulation system.

To handle collision of deformable objects, there are two classes of methods: Penalty Methods and Constraint Methods. Penalty methods lack physical plausibility and require the definition of a stiffness constant  $k$  for each collision, while the constraint method is a linear complementary problem that is solved by iterative methods. Thus, the resulting methods tend to be expensive or sensitive to numerical problems and require more effortful implementations (25). We propose a hybrid method that combines the accuracy and physical correctness of constraint methods with the simplicity and efficiency of penalty methods by applying an impulse force:

$$F_i = \frac{m_i}{\Delta t^2} \sum_{n=0}^K d_i^n$$

where  $m_i$  represents the mass of  $i$ th mass point,  $\Delta t$  is the time step,  $d_i^n$  is the penetration depth that mass point  $i$  is relative to vascular triangle  $n$ .

## Control system

Figure 9 shows a block diagram of the whole control scheme of the CIS system. In the control system, visual manipulation is advanced in accordance with a surgeon's operation and obtained by tracking devices (sensors). On one hand, the computer will calculate whether there is mechanical collision between the interventional instruments and the blood vessels, and then display the reconstructed 3D vascular model on the screen. On the other hand, the tracking device will measure the displacement and angles, and then calculate the forward kinematics to obtain the position and orientation and deliver this to the processing module. The data are then transmitted to stepper motors for calculation of the inverse kinematics, which generates force feedback to the operator. The User Datagram Protocol (UDP) communication rate between sensors and the processing module is confined to 100 Hz (26), while the servo-frequency of the feedback control system is updated to 950 Hz. Hence, the data of the inverse kinematics are interpolated to ensure the continuity of force feedback.

In this platform, the two important factors that crucially affect the system performance are position and rotation. Figure 10 depicts the detailed block diagram of the control system. Position control is achieved using a Proportional-Integral-Derivative (PID) controller, whose input is the difference between the actual position and the position detected from the tracking device. A feed-forward loop is applied to improve the accuracy of the position and to

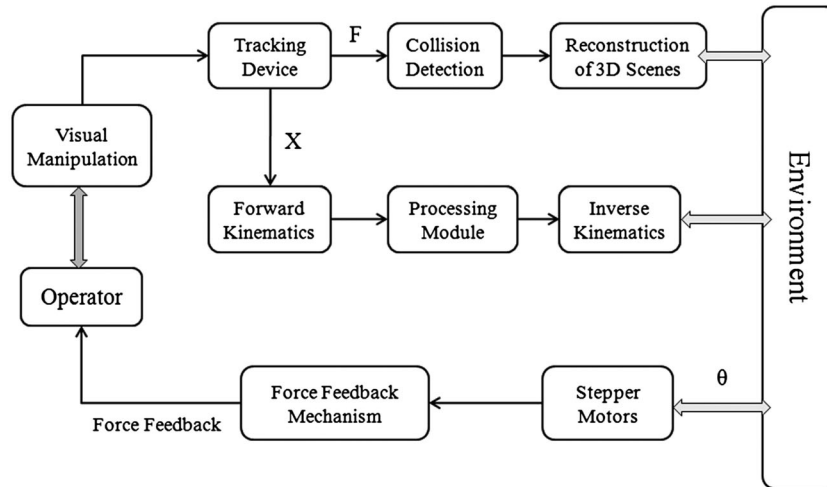


Figure 9. Block diagram of the whole control scheme of the CIS system

accelerate the response. Then, the signals are amplified and delivered to the processing module to compute the actual position. In addition, the rotation of the guidewire is especially important when it is advanced from the aorta to the artery branches. Therefore, appropriate rotation is crucial to the success rate of the surgery, and also greatly reduces the operation time and the occurrence of complications. The tracking device detects changes in the surgical environment, such as visual manipulation and human operation, and simultaneously captures and displays them on the screen.

Our simulation system has been demonstrated to be physically accurate and robust. More importantly, it must also be efficient to run in real-time. Table 3 summarizes the computational time for handling collision, adaptive sampling, physics computation and rendering with different number of nodes. The experiment demonstrates that our system's time complexity is linear with respect to the number of nodes and yet can easily perform the simulation in real-time at 75 fps.

Table 3. Computation time with different nodes in our simulation system (milliseconds)

Number of nodes	Handling collision	Adaptive sampling	Physics computation	Rendering	Total time
100	0.66	0.02	1.01	2.03	5.56
200	0.93	0.03	2.11	2.43	8.14
300	1.11	0.04	3.13	2.96	10.98
380	1.92	0.05	3.97	3.51	12.89

## Experimental results

### Preliminary system evaluation

The performance of the CIS simulation system was evaluated using translational and rotational calibration tests. Four subjects were divided into two groups (untrained interventionist, UI, and trained interventionist, TI) from the professional field involved in the experiments. The tag-marked interventional instrument was used in the

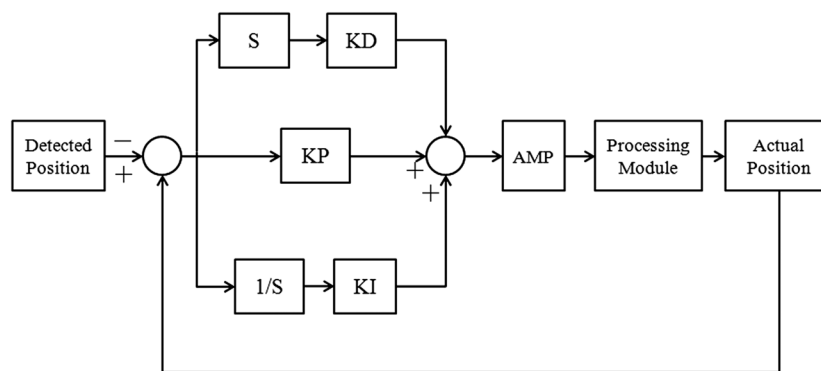


Figure 10. Detailed block diagram of control system



translational calibration test, and manipulated by the participants at a uniform scale. Moreover, the error of rotation calibration test was evaluated using a disk scale mounted on the mechanical system. The tests were performed mechanically with the same calibration methods to compare the differences between the two groups. In all of the following experiments, each experiment was repeated three times to obtain an average. All data and videos for analysis were auto-collected with a pre-designed program. Tests designed for preliminary system evaluation included the translation test and the rotation test.

#### Translation test

In this test, we aimed to quantify the accuracy between UI and TI. As hand-tremor is an important factor affecting the calibration accuracy, we evaluated the filtering effect using an average. The participants were asked to advance the interventional instrument at a uniform scale (60 cm) and finish the test within 120 s. During the test, the axial displacement was measured by optical sensors and compared with the distance between two marks. The deviation was calculated as the root-mean square error (RMSE).

#### Rotation test

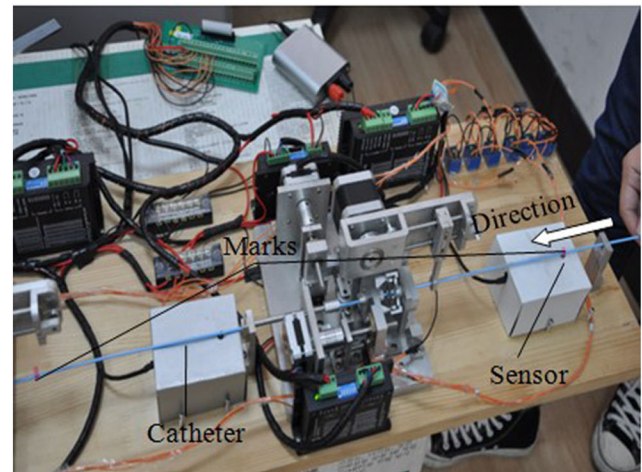
Similarly, the participants were required to rotate the instruments on the dial. The evaluation standard was using the RMSE against the actual cylinder numbers and the recording cylinder numbers registered by the optical sensors.

Figure 11 illustrates the definitions of the translation test and the rotation test. The axial displacement accuracies of the UI team and the TI groups were approximately 0.6 and 0.3 mm, respectively (Figure 12(a)). Thus, the rotation accuracy improved by almost 50% after the interventionist received trained in this platform. Our system has a higher accuracy than a similar system designed by Wangsheng Lu (27) (0.5 mm). In addition, the rotation accuracy of the TI group improved by 32.5% compared with the UI group (Figure 12(b)). In both tests, the deviation errors of the TI group were much smaller than the UI group, indicating that skill training for interventionists was beneficial to alleviating the effects of difference in individual experience and improving the operational accuracy.

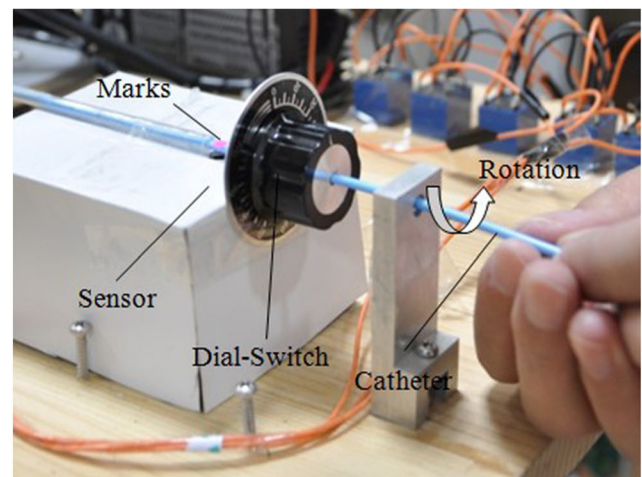
## Simulation study

### Simulation experiment

Simulation experiments were performed on the developed system to simulate the CIS procedure. Three experiments were conducted: (a) angiographic catheter simulation; (b) guiding simulation; (c) coronary dilatation catheter simulation. Angiographic catheter (size 6F, 534-621 T,



(a)



(b)

Figure 11. Definition of translation test (a) and rotation test (b)

2 mm × 100 cm) purchased from Miami Lakes (USA), guidewire (Standard J-TIP, 502-521, 0.89 mm × 150 cm) from Cordis Corporation (USA) and Voyager RX coronary dilatation catheter (1011398-15, 3.50 mm × 15 mm, 143 cm) from Abbott Vascular Santa Clara were used.

Simulation (a) is a necessary CIS procedure as the interventionist in preparing an operation channel. The accuracy of the force feedback is the most difficult to measure but significant part of the surgery, and also affects the surgical quality. Inserting the guidewire requires much more frequent changes of the rotating tip's orientation as well as a longer time. Thus, simulation (b) was designed to simulate the actual operation process using the developed system to train trainees with professional skills. Then, the results were compared to the actual surgery operated by an experienced expert in accordance with the completion time. However, simulation (c) was expected to simulate the percutaneous transluminal coronary angioplasty in

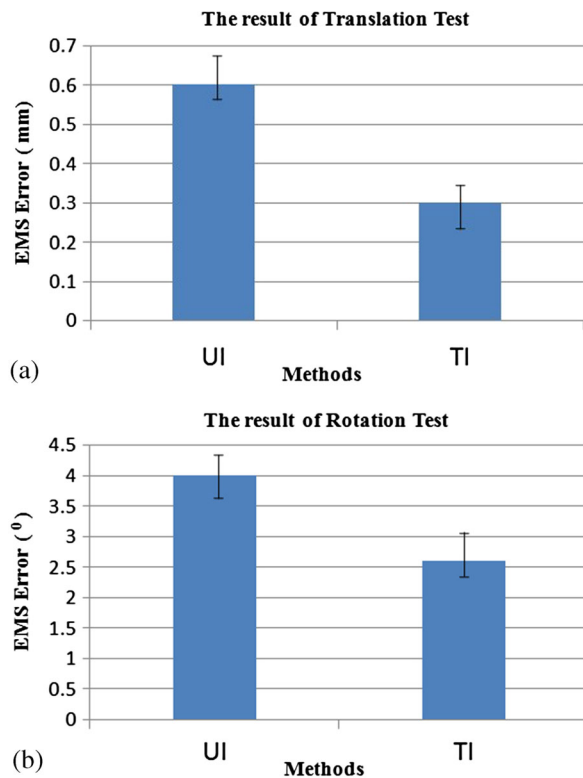


Figure 12. Results of translation test (a) and rotation test (b)

the patient's blood vessels. The interventionist is also an expert cardiologist with 15 years of clinical experience. Each subject was asked to conduct the simulation three times before each simulation experiment.

### Angiographic catheter simulation

This simulation was successfully performed on the robotic system (Figure 13(a)) and Figure 13(b) shows the user interface of the platform. The catheter was inserted quickly and smoothly into the selected simulated branch vessels. The speed of the catheter is approximately 10–30 mm/s, which satisfies the clinical demands of VIS. The maximum (30 mm/s) was preferred when the catheter was moved

through a large blood vessel far away from the lesions, while the minimum (10 mm/s) was selected when in a smaller blood vessel close to the lesions. The whole procedure took approximately 1 min.

### Guidewire simulation

Figure 14 shows the results of the successful simulation of the guidewire. As mentioned above, the guidewire simulation is the most difficult manipulation in a small space with high accuracy. This simulation is divided into three sections for comparing the operation time with manual operation in an actual operation. The sections are described as follows:

*Section 1, motion in selected blood vessel: from the insertion point to the corner of the aorta*

*Section 2, motion in the aorta: from the corner of the aorta to a suitable inflection point in the branch vessel*

*Section 3, motion in the branch vessel: from the branch vessel to the lesions.*

Table 4 shows a comparison of completion times between the simulation and manual operation. Each completion time is an average of three experiments. Despite the differences in experiment conditions, the required time of each section is shown in the result. Obviously, Section 2 was the most time-consuming and required highly precise operation, while sections 1 and 3 needed relatively faster motion and less time.

The total time of simulation was almost double that of the manual operation, but the contribution ratios to each section were not obviously different between simulation and manual operation. A shorter time was expected to finish section 3 in such a small space, but this problem could be solved only by positive rotation with high accuracy. Moreover, the reason for such a long time was most attributed to the system's insufficient dexterity. Our training platform was not easy-to-use so that the completion time was prolonged. Therefore, we should enhance the interaction of the user interface and the system dexterity without sacrificing system accuracy. Also high-frequency updating for the control system could shorten the total time. In the

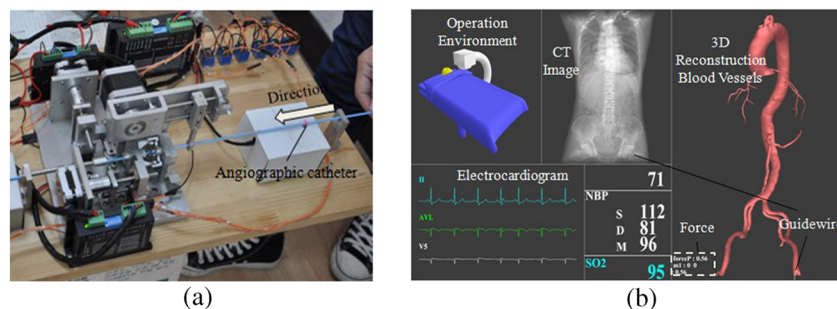


Figure 13. Angiographic catheter simulation (a) and the user interface (b)

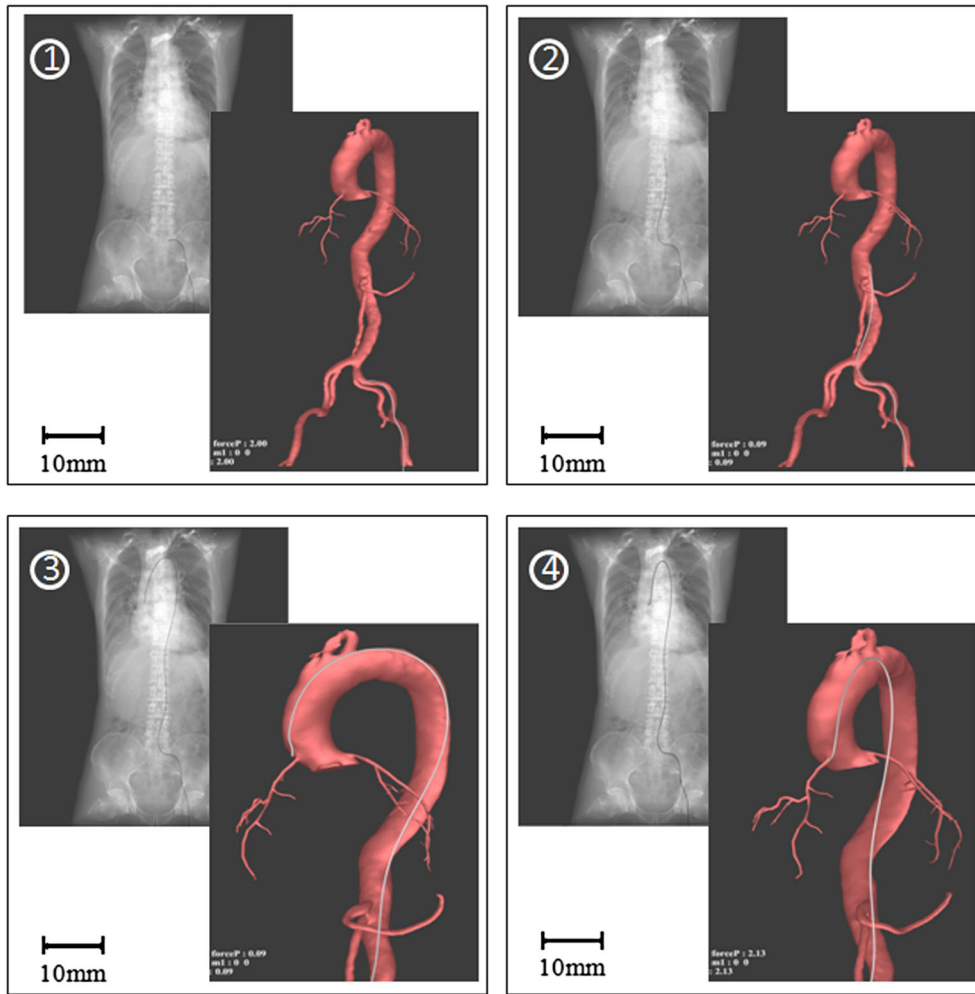


Figure 14. Results of guidewire simulation

Table 4. Comparison of complete time: simulation and manual operation

Section no.	Simulation operation		Manual operation		Increase (s)
	Time (min)	Ratio (%)	Time (min)	Ratio (%)	
1	0.35	5.8	0.15	4.1	12
2	0.15	2.5	0.1	2.9	3
3	5.5	91.7	3.35	93.0	129
Total	6	1	3.6	1	144

future, we want to assure that whether a longer completion time of the robotic simulation operation is acceptable for the real clinical surgery.

### Coronary dilatation catheter simulation

Coronary dilatation catheter simulation was successfully performed and the results are shown in Figure 15. In this

simulation, while the guidewire was kept motionless, the coronary dilatation catheter was inserted quickly and steadily into the lesions and the stent placement of the simulating operation was finally completed. The total procedure took approximately 2 min.

These results confirm that the platform was sufficient to simulate the complex CIS procedure with high accuracy. We consider the platform to be suitable for performing the actual surgery. Nevertheless, the total completion time was much longer than the manual operation, and thus a more dexterous system with a more user-friendly interface and better control system is needed to improve the system's performance.

### Discussion

This paper described a CIS real-time virtual training platform integrated with haptic device for training core techniques for



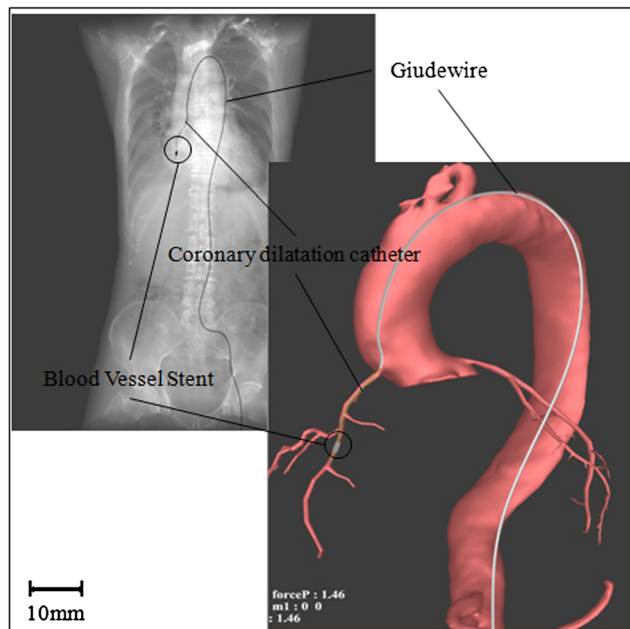


Figure 15. Results of coronary dilatation catheter simulation

trainees. It consists of a mechanical manipulation unit, a simulation platform and a user interface. The decoupled haptic device offers a superior dynamic behavior and low inertia of the force feedback, which delivers a realistic simulation environment to the trainees. The simulation platform allows for the testing of VIS principles, such as guidewire and catheter simulation and stent placement, as well as rendering techniques for realistic simulation.

To preliminarily evaluate the platform, we performed translational and rotational tests between the UI and TI groups. The results showed that their accuracies improved by 50% and 32.5%, respectively for the two tests, after using the virtual training platform. This indicated that this platform was beneficial to young inexperienced interventionists and that the system is robust. The rotation test showed that the deviation error of the TI group was much smaller than the UI group, indicating that it could be beneficial to alleviating the influence of the effects for the individual experience. We conducted an angiographic catheter simulation, a guiding simulation and a coronary dilatation catheter simulation to simulate the whole procedure. The results showed that the completion time was longer with the simulation operation, which was the biggest drawback of the platform. Thus, shortening the total completion time will need to be accomplished. Another problem was to obtain flexible and clinically-suitable force feedback. Further experimental analysis will be employed in the future to address this issue. However, the platform was acceptable for clinical operation and several experienced surgeons have reported being satisfied with the platform because of its realistic simulated force feedback, and has potential for being a good virtual training platform for CIS virtual training.

## Conclusions

The CIS virtual training platform was elaborated in this study. We successfully performed a complex CIS procedure with sufficient accuracy, utilizing a friendly user interface and receiving reasonable force feedback. It may be a potential method for virtual training.

In future studies, we should also improve the flexibility, accuracy and response of the mechanical system in order to shorten the total completion time. In addition, a complete skill education and training system for young interventionists is particularly important, and can improve the platform's overall quality. Furthermore, a validation study will be performed to test the system's performance in the future.

## Acknowledgements

The authors acknowledge funding from the Major Project of Natural Science Foundation of China (Grant No.61190124, No.61190120), the Natural Science Foundation of China (Grant No.61311140171, No.60873131), the Key Project of National Science and Technology Foundation of China (Grant No.2009BAI71B06), the High Technology Research and Development Program (Grant No.2006AA01Z310, No.2009AA01Z313) and the Program of Medicine and Engineering Cross Fund of Shanghai Jiao Tong University (Grant No.YG2012MS54, No.YJ2013ZD03). We also thank Zilong Deng and Jun Jiang for assisting in this study.

## Conflict of interest

The authors have stated explicitly that there are no conflicts of interest in connection with this article.

## References

1. Valji K. *Vascular and Interventional Radiology*. W.B. Saunders: Philadelphia, PA, 1999.
2. Rebolz CM, Reynolds K, Wofford MR, et al. Effect of soybean protein on novel cardiovascular disease risk factors: a randomized controlled trial. *Eur J Clin Nutr* 2013; **67**(1): 58–63.
3. Merrill GM, inventor; HT Medical Systems, Inc., assignee. Interventional radiology interface apparatus and method. United States patent US 6106301, August 2000.
4. Ohlsson F, inventor; Mentice AB, assignee. Interventional simulation device. United States patent US 7520749B2, April 21 2009.
5. Bronstein R, Israeli S, inventors; Symbionix Ltd., assignee. Medical simulation device with motion detector. United States patent US2007/0134637A1, June 14 2007.
6. Bronstein R, Niv F, Ofek S, inventor; Massachusetts Institute of Technology, assignee. System and method for performing computerized simulations for image-guided procedures using a



- patient specific model. United States patent US006134003A, Oct 17 2000.
7. Moix T, Ilic D, Fracheboud B, *et al.* A real-time haptic interface for interventional radiology procedures. *Med Meets Virtual Reality* 2005; **111**: 329–333.
  8. Moix T, Ilic D, Bleuler H, *et al.* A haptic device for guide wire in Interventional Radiology procedures. *Med Meets Virtual Reality* 2006; **119**: 388–392.
  9. Ilic D, Moix T, Cullough NMC, *et al.* Real-time haptic interface for VR colonoscopy simulation. *Med Meets Virtual Reality* 2005; **111**: 208–212.
  10. John NW, Luboz V, Bello F, *et al.* Physics-based virtual environment for training core skills in vascular interventional radiological procedures. *Med Meets Virtual Reality* 2008; **132**: 195–197.
  11. Luboz V, Hughes C, Gould D, *et al.* Real-time Seldinger technique simulation in complex vascular models. *Int J CARS* 2009; **4**: 589–596.
  12. Wang F, Duratti L, Samur E, *et al.* A computer-based real-time simulation of interventional radiology. In Proceedings of the 29th Annual International Conference of the IEEE EMBS, France, 2007; 1742–1745.
  13. Cotin S, Dawson SL, Meglan D, *et al.* ICTS, an interventional cardiology training system [serial on the internet]. 2002 [cited 2014 Apr 14]; Available from: [https://www-sop.inria.fr/teams/asclepios/Publications-tracked/Delingette/MMVR2000\\_paper](https://www-sop.inria.fr/teams/asclepios/Publications-tracked/Delingette/MMVR2000_paper).
  14. Luboz V, Blazewski R, Gould D, *et al.* Real-time guidewire simulation in complex vascular models. *Int J Comput Assisted Radiol Surg* 2009; **4**(6): 589–596.
  15. Alderliesten T, Bosman PA, *et al.* Towards a real-time minimally-invasive vascular intervention simulation system. *Med Imaging* 2007; **26**(1): 128–132.
  16. Lenoir J, Cotin S, Duriez C, *et al.* Interactive physically-based simulation of catheter and guidewire. *Comput Graph* 2006; **30**(3): 416–422.
  17. Duratti L, Wang F, Samur E, *et al.* A real-time simulator for interventional radiology. In Proceedings of the 2008 ACM symposium on virtual reality software and technology, Bordeaux, 2008; 27–29.
  18. Ganji Y, Janabi-Sharifi F. Kinematic characterization of a cardiac ablation catheter. In Proceedings of the IEEE/RSJ International Conference on Intelligent Robots and Systems (IROS), California, 2007; 1876–1881.
  19. Ganji Y, Janabi-Sharifi F. Catheter kinematics for intracardiac navigation. *Biomed Eng* 2009; **56**(3): 621–632.
  20. Tang W, Lagadec P, Gould D, *et al.* A realistic elastic rod model for real-time simulation of minimally invasive vascular interventions. *Visual Comput* 2010; **26**(9): 1157–1165.
  21. Luo Z, Cai J, Wang S, *et al.* Magnetic navigation for thoracic aortic stent-graft deployment using ultrasound image guidance. *Biomed Eng* 2013; **60**(3): 862–871.
  22. Tan H, Eberman B. Human factors for the design of force-reflecting haptic interfaces. *Dynam Syst Control* 1994; **55**(1): 353–359.
  23. Bergou M, Wardetzky M, Robinson S, *et al.* Discrete elastic rods. *ACM Trans. Graph* 2008; **27**(3): 63.
  24. Klosowski JT, Held M, *et al.* Efficient collision detection using bounding volume hierarchies of k-DOPs. *Visualiz Comput Graph* 1998; **4**(1): 21–36.
  25. Spillmann J, Becker M, Teschner M, *et al.* Non-iterative computation of contact forces for deformable objects. *J WSCG* 2007: 1–8.
  26. Mitsuishi M, Morita A, Sugita N, *et al.* Master–slave robotic platform and its feasibility study for micro-neurosurgery. *Int J Med Robotics Comput Assist Surg* 2013; **9**: 180–189.
  27. Lu WS, Xu WY, Zhang J, *et al.* Application study of medical robots in vascular intervention. *Int J Med Robotics Comput Assist Surg* 2011; **7**: 361–366.

## Supporting information

Additional supporting information may be found in the online version of this article at the publisher's web-site.